

Marcella Martignoni · Ruben de Kanter  
Anna Moscone · Pietro Grossi · Mario Monshouwer

## Lack of strain-related differences in drug metabolism and efflux transporter characteristics between CD-1 and athymic nude mice

Received: 12 May 2004 / Accepted: 23 July 2004 / Published online: 22 September 2004  
© Springer-Verlag 2004

**Abstract** CD-1 mice are commonly used in oncology metabolism and toxicity to support drug discovery and development and to examine drug metabolism and toxicity properties of new chemical entities. On the other hand, athymic nude mice are the preferred animals to investigate tumor growth inhibition. Therefore, a frequently asked question is: are the metabolic and pharmacokinetic characteristics of xenobiotics in these two mouse strains comparable or not? To address this issue, we characterized drug metabolism and efflux transporter properties in both strains and in different organs. The metabolic stability of a set of 20 compounds and metabolite formation of cytochrome P450 (CYP) marker substrates (testosterone, ethoxyresorufin and pentoxyresorufin) were measured in liver microsomes. Drug conjugation was studied by following the disappearance of 7-hydroxycoumarin and the formation of its glucuronide and sulfate conjugates in freshly prepared liver slices. In addition, mRNA expression levels of the main cyp genes and drug efflux transporters were investigated by real-time RT-PCR in the liver, kidney, intestine and adrenal glands. No significant differences in enzymatic activities and metabolite formation were observed between the two strains. Also mRNA expression profiles of cyp and drug transporter genes were similar between CD-1 and nude mice.

**Keywords** Athymic nude mice · CD-1 mice · Cytochrome P450 · Strain differences · Transporter proteins

**Abbreviations** BSA: Bovine serum albumin ·  $CL_{int}$ : Intrinsic metabolic clearance · CYP: Cytochrome P450 · DMSO: Dimethylsulfoxide · dATP: 2'-Deoxyadenine 5'-triphosphate · dCTP: 2'-Deoxycytosine 5'-triphosphate · dGTP: 2'-Deoxyguanine 5'-triphosphate · dNTP: 2'-Deoxynucleoside 5'-triphosphate · dTTP: 2'-Deoxythymine 5'-triphosphate · EROD: 7-Ethoxyresorufin-*O*-deethylase · 7-HC: 7-Hydroxycoumarin · LPS: Lipopolysaccharide · mdr1a/1b: Multidrug resistance 1a/1b · mrp1/2: Multidrug resistance associated protein 1/2 · LC-MS/MS: Liquid chromatography coupled to tandem mass spectrometry · [S]: Substrate concentration · PROD: 7-Pentoxoresorufin-*O*-dephenylase · TOH: Testosterone hydroxylase

### Introduction

Among the animals used in research, mice comprise the majority of all experimental mammals. The remarkable genetic similarity between mice and humans, combined with their small size, makes the mouse a preferred experimental animal model within cancer drug discovery and development. Specially bred mice, with natural or introduced genetic deficiencies have provided a wide range of genetic mouse models of human diseases [8]. An example is the athymic nude mouse (nu/nu), which has an unusually low immune response. These mice are born without a thymus gland and therefore cannot generate mature T lymphocytes and are unable to mount most types of immune response. Their immunodeficient status allows a variety of human tumors to be grafted without rejection allowing the investigation of tumor growth inhibition of potential antitumor agents [9].

Parallel to in vivo screening for identifying pharmacologically active and potent antitumor compounds,

M. Martignoni (✉) · R. de Kanter · A. Moscone  
P. Grossi · M. Monshouwer  
Pharmacokinetics, Dynamics and Metabolism,  
Pharmacia Italy, Pfizer Group, Inc.,  
Viale Pasteur 10, 20014 Nerviano, MI, Italy  
E-mail: marcella.martignoni@nervianoms.com  
Tel.: +39-331-581228  
Fax: +39-331-581105

in vivo studies are performed to evaluate the safety and pharmacokinetic properties of drug candidates [20]. The pharmacokinetic information of potential antitumor compounds obtained from studies in CD-1 mice is often used to design appropriate dose regimens for these compounds in tumor-bearing nude mice. However, neither strain is well characterized with respect to its drug metabolism and drug transporter characteristics. Therefore, information on possible strain differences between CD-1 and athymic nude mice which may affect the drug disposition of new chemical entities would be extremely useful. Both drug metabolism and drug transporters are important features that determine the disposition of drugs. The liver is the primary site for drug metabolism and contains the necessary enzymes for metabolism of drugs and other xenobiotics. These enzymes induce two metabolic pathways: phase I (functionalization) and phase II (biosynthetic) metabolic reactions [19]. Some typical examples of phase I metabolic reactions include oxidation and hydrolysis mediated by cytochrome P450 (CYP). Phase II metabolic reactions involve the introduction of a hydrophilic endogenous species, such as glucuronic acid or sulfate, to the drug molecule. The elimination of a drug by transport proteins, referred to as drug transporter enzymes, as phase III metabolism [21], has attracted increasing interest recently. These enzymes are expressed in many tissues such as intestine, liver, kidney, and brain, and play key roles in drug absorption, distribution, and excretion [1, 12]. Modulation of drug metabolism, but also of drug transporters may increase the risk of toxicity and other adverse drug reactions.

To gain an insight into possible strain-related differences in drug metabolism and drug transporters between CD-1 and athymic nude mice, we characterized both phase I-mediated and phase II-mediated hepatic drug metabolism as well as the major drug efflux transporters (phase III). Phase I activities were investigated by studying the metabolic stability of a set of 20 compounds at low concentrations and by measuring metabolite formation of well-known marker substrates of phase I metabolism (ethoxyresorufin, pentoxyresorufin, and testosterone) using liver microsomes. Phase II metabolism, in freshly prepared mouse liver slices, was evaluated using 7-hydroxycoumarin (7-HC) as a marker substrate for sulfation and glucuronidation. In addition, expression profiles of major mouse cyp isoforms and efflux transporters were determined in several organs, by measuring quantitatively mRNA levels using real-time RT-PCR. The mouse cyp genes included in this study were *cyp1a1*, *cyp1a2*, *cyp2b10* and *cyp3a11*. The efflux transporters *mdr1a*, *mdr1b*, *mrp1* and *mrp2* were included in the current study because of their important protective and secretory roles in affecting the hepatobiliary, renal or intestinal elimination of several drugs [2, 16, 17].

## Materials and methods

### Chemicals

The following compounds were obtained from the sources indicated. 7-HC, 7-HC glucuronide, DMSO, D-glucose, gentamicin sulfate, ethoxyresorufin, pentoxyresorufin, midazolam, ketoconazole, quinidine, sulfaphenazole, chlorpromazine, lansoprazole, orphenadrine, salmeterol, fluoxetine, nifedipine, warfarin, dextromethorphan, fluphenazine, erythromycin, tolbutamide, verapamil, carbamazepine and resorufin were from Sigma-Aldrich (St Louis, Mo.). Testosterone was from Fluka (Buchs, Switzerland). 7-HC sulfate and testosterone metabolites were from Ultrafine Chemicals (Manchester, UK). Indinavir, delaviridine and triazolam were from Pharmacia (Kalamazoo, Mich.). Williams' Medium E, 5× first strand buffer, RNaseOUT, Superscript, dATP, dGTP, dCTP, dTTP, random hexamer primers, DTT and BSA were obtained from Gibco (Paisley, UK). RNA 6000 Nano Assay was from Agilent Technologies (Palo Alto, Calif.). RiboGreen RNA quantitation kit was from Molecular Probes (Eugene, Ore.). Qiagen RNAeasy minikit was from Qiagen (Crawley, UK). RNAlater was from Ambion (Austin, Tx.). TaqMan Universal PCR Master Mix Reagents, SYBR Green PCR Master Mix, Assays-on-Demand Gene Expression product and TaqMan probes were obtained from Applied Biosystems (Foster City, Calif.). The oligonucleotide primers were synthesized by Pharmacia Laboratories (Nerviano, Milano, Italy).

### Animals

Male CD-1 mouse and male nude mice were obtained from Charles River (Como, Italy) aged 8–10 weeks, and were maintained under a 12-h light/dark cycle, with free access to drinking water. Nude mice were fed with  $\gamma$ -irradiated 4RFN food pellets that are richer in proteins and lipids, while CD-1 mice received standard 4RF21 pellets (Mucedola, Settimo Milanese, MI, Italy). Mice were housed in standard cages and bedding but for nude mice the air supply was filtered using EPA filters to protect them against infections.

### Liver microsome preparation

Three CD-1 and three nude mice were killed by cervical dislocation and the livers immediately excised. Small samples of liver were snap-frozen in liquid nitrogen and stored at  $-80^{\circ}\text{C}$  before homogenization in 25 mM phosphate-buffered saline, pH 7.4, using a Potter homogenizer. Microsomes were prepared by ultracentrifugation (100,000 *g* for 1 h) of the postmitochondrial

supernatant (9000 g for 20 min). The microsomal pellet was resuspended in homogenization buffer and centrifuged twice at 100,000 g for 60 min. The washed microsomes were suspended in 0.1 M Tris buffer (pH 7.4), containing 20% (w/v) glycerol, so that 1 ml of microsomal suspension was equivalent to approximately 1 g original wet weight of thawed liver. Microsomes were aliquoted and stored at  $-80^{\circ}\text{C}$ . The protein concentration was determined using the method of Bradford [3].

### Metabolic stability

The compounds (testosterone, midazolam, chlorpromazine, nifedipine, verapamil, lansoprazole, delaviridine, dextromethorphan, indinavir, ketoconazole, orphenadine, triazolam, fluphenazine, quinidine, salmeterol, warfarin, sulfaphenazole, erythromycin, tolbutamide and fluoxetine) were dissolved in DMSO at 10 mM. These stock solutions were diluted with acetonitrile to lower the DMSO concentration because it is known that DMSO inhibits microsomal enzyme activities [4]. Incubations were performed in 20 mM phosphate buffer at pH 7.4 for 45 min in the presence of microsomes and 2  $\mu\text{M}$  of substrate at  $37^{\circ}\text{C}$ . The total concentration of organic solvent was 0.75%, of which 0.13% was DMSO. As a cofactor NADPH was added at 1 mM. The total incubation volume was 300  $\mu\text{l}$ . The reactions were started by the addition of microsomes (final concentration: 0.5 mg protein/ml) and terminated by the addition of 100  $\mu\text{l}$  ice-cold acetonitrile containing 7  $\mu\text{M}$  carbamazepine as internal standard. All incubations were performed in duplicate using an automated liquid handling system (MultiProbe, Packard). Analysis was performed using LC-MS/MS, as described previously [10]. Quantification was performed by comparing the peak areas with those of authentic standards of each metabolite. The percentage of the substrate remaining was calculated relative to control (heat-inactivated) microsomes.

### Metabolite formation incubation

Testosterone, ethoxyresorufin and pentoxyresorufin were dissolved in DMSO. Incubations were performed in 20 mM phosphate buffer, pH 7.4, for either 10 min (ethoxyresorufin and pentoxyresorufin) or 30 min (testosterone) in the presence of microsomes (1 mg protein/ml) at  $37^{\circ}\text{C}$ . Substrate concentrations were 0.25 mM for testosterone and 5  $\mu\text{M}$  for 7-ethoxyresorufin-*O*-deethylase (EROD) and for 7-pentoxyresorufin-*O*-deethylase (PROD). The final DMSO concentration was 0.5%. As a cofactor, NADPH was added at 1 mM. The total incubation volume was 1 ml. All incubations were performed in triplicate. The testosterone metabolites were analyzed by HPLC with UV detection [10] while the formation of resorufin from ethoxyresorufin and pentoxyresorufin was detected by fluorimetry at 530 nm

excitation and 590 nm emission, using authentic standards.

### Liver slice preparation

After intraperitoneal anesthesia with a cocktail of ketamine (67 mg/kg), xylazine (15 mg/kg) and acepromazine (1 mg/kg), livers were removed and stored in cold Williams' medium E until use (maximum 30 min). Liver cores and slices (diameter 8 mm, wet weight about 15 mg) were prepared in ice-cold Williams' medium E that was oxygenated with 95%  $\text{O}_2$ /5%  $\text{CO}_2$  and supplemented with extra glucose (final concentration 25 mM), using a Krumdieck tissue slicer as described previously [10]. The slices obtained were subsequently stored in ice-cold Williams' medium E until use (within 1 h of preparation).

### Culture of liver slices

Slices were individually incubated in six-well culture plates (Falcon, France) in 2.0 ml Williams' medium E under 95%  $\text{O}_2$ /5%  $\text{CO}_2$  (one slice per well) at  $37^{\circ}\text{C}$  while shaking horizontally 90–100 times  $\text{min}^{-1}$ . The culture medium consisted of Williams' medium E containing glucose (25 mM) and gentamicin (50  $\mu\text{g/ml}$ ).

CD-1 and nude mouse liver slices were incubated in triplicate with either 1  $\mu\text{M}$  or 50  $\mu\text{M}$  7-HC for 3 h. Prior to the immersion of the slices, 7-HC was added to the incubation medium as a 1000 times concentrated solution in methanol. At different time points (0, 30, 60, 90, and 180 min) an aliquot of the medium was removed and the reaction stopped by adding an equal volume of acetonitrile and stored at  $-20^{\circ}\text{C}$ . The samples were analyzed using LC-MS/MS as described previously [10]. The slices were disrupted using an MSE ultrasonic disintegrator (Fisons, Loughborough, UK) in their own incubation medium for the determination of the protein content using the method of Bradford [3].  $\text{CL}_{\text{int}}$  was determined from the disappearance of the parent compound as described previously [7].

### RNA preparation from liver, kidney, adrenal glands and intestine samples

Tissue samples (about 30 mg) of liver, kidney, adrenal glands, duodenum, ileum and colon of both strains were taken from three male nude mouse and three male CD-1 mouse after anesthesia, as described above, and stored in RNAlater at  $4^{\circ}\text{C}$ . Total RNA was extracted from the tissue using QIAGEN RNeasy minikits. The quality of the isolated RNA was assessed using the RNA 6000 Nano Assay and the Agilent 2100 bioanalyzer. RNA concentrations were determined using a RiboGreen RNA quantitation kit.

## Reverse transcription

The reaction mixture (final volume 40  $\mu$ l) was prepared with final concentrations as follows: 1 $\times$  first-strand buffer, 64 U RNaseOUT, 200 U Superscript, 0.6 mM dNTP (dATP, dGTP, dCTP and dTTP), 0.75  $\mu$ g random hexamer primers, 10 mM DTT and 16 ng BSA. To this mixture was added 1  $\mu$ g total extracted RNA. The reverse transcription reaction was performed for 10 min at 25°C, 60 min at 42°C and 30 min at 37°C.

## Design of primers and probes

The cDNA sequences of mouse *cyp1a1*, *cyp1a2*, *cyp3a11* and  $\beta$ -actin were obtained from GenBank (accession numbers: NM 009992, NM 009993, NM 007818 and NM 007393). Taqman primer and probe sets for *cyp2b10* have been described previously [14]. PCR primers and probe sequences were designed using PrimerExpress software (Applied Biosystems) and are shown in Table 1. Nucleotide primers and probe sequences were checked against the NCBI BLAST database to ensure specificity for the selected gene. The Taqman primer and probe sets for *mdr1a*, *mdr1b*, *mrp1* and *mrp2* were bought from Applied Biosystems (Assays-on-Demand Gene Expression product Mm 00440761m1, Mm 00440736m1, Mm 00456156m1 and Mm 00496899m1).

## Real-time quantitative PCR

Real-time quantitative PCR was performed, employing an iCycler iQ real-time PCR detector system (Bio-Rad). The PCR reaction was performed in a 96-well plate. The reaction mixture (13.5  $\mu$ l) was added to each well to give the following concentrations: 1 $\times$  master mix reagents, either 200–900 nM of each primer and 200 nM probe for each *cyp* mRNA assay or 1 $\times$  Assay-on-Demand Gene Expression Assay Mix for

transporter mRNA assay. cDNA (1.5  $\mu$ l) was added to each well and the final volume was 15  $\mu$ l. The thermal cycle conditions were 50°C for 2 min, 95°C for 10 min to activate Amplitaq Gold DNA polymerase, denaturation at 95°C for 15 s and annealing/extension at 59°C for 1 min (40 cycles). Quantitative PCR for  $\beta$ -actin mRNA was also performed to normalize for RNA loading.

## Statistical analysis

Differences among group mean values were assessed by Student's *t*-test. *P* values <0.05 were considered statistically significant.

## Results

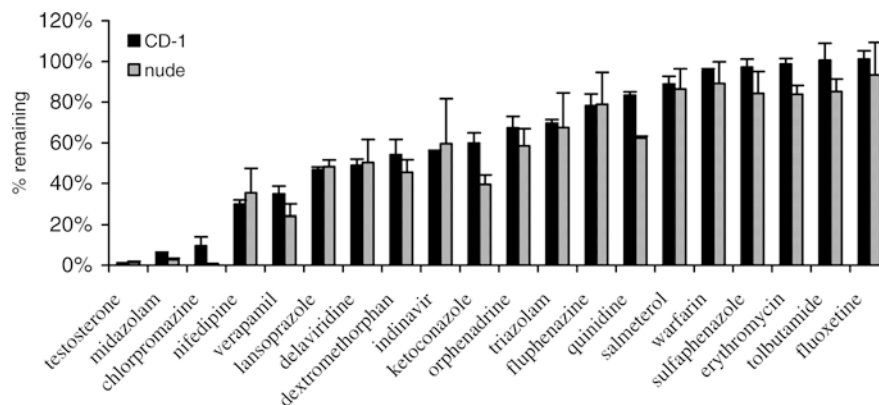
### Comparison of metabolic stability in liver microsomes from mice

The metabolic stabilities of a set of 20 compounds incubated with liver microsomes prepared from CD-1 and nude mice are presented in Fig. 1. The set of compounds was selected to cover a wide range of metabolic stabilities, from unstable to stable under the defined conditions. The metabolic stability experiments were performed at low substrate concentrations (2  $\mu$ M). Using such a low substrate concentration ([S]), and assuming that [S]  $\ll$  *K<sub>m</sub>*, the disappearance of the substrate will follow first-order kinetics and as a result the metabolic stability data would be a direct indication of hepatic CL<sub>int</sub> [7]. As shown in Fig. 1, there was a remarkable similarity in metabolic stabilities between the two strains. Despite the fact that ketoconazole, quinidine and chlorpromazine were found to be slightly more stable in liver microsomes prepared from CD-1 mice, the general the rank order of compounds from unstable to stable was very similar between the two mouse strains studied.

**Table 1** Taqman primer and probe sequences of mouse *cyp* mRNA

Gene	Primers/probes	5' $\rightarrow$ 3' sequence	Amplicon size (bp)
<i>cyp1a1</i>	Forward	ATAAGGTCATCACGATTGTTTTGG	84
	Reverse	GGTACATGAGGCTCCACGAGAT	
<i>cyp1a2</i>	Forward	CACAGTCACAACTGC	143
	Reverse	CGTCAGCAAGCTTCAGAAGG	
<i>cyp2b10</i>	Forward	CGATGTTTCAGCATCTCCTCG	70
	Reverse	CCAAAGCACATGGCACCAATGAC	
<i>cyp3a11</i>	Forward	CAGGTGATCGGCTCACACC	64
	Reverse	TGACTGCATCTGAGTATGGCATT	
$\beta$ -Actin	Forward	ACCAACCCTTGATGACCGCACCA	75
	Reverse	TCACACACAGTTGTAGGGAGAA	
	Probe	GTCCATCCCTGCTTGTTTGTG	
	Probe	ACAGAGAAGTAAATTGC	
	Probe	TTCTTTGCAGCTCCTTCGTT	
	Reverse	GACCAGCGCAGCGATATC	

**Fig. 1** Metabolic stability (expressed as percent remaining) of 20 drugs after incubation with liver microsomes obtained from CD-1 and nude mice. The data presented are means  $\pm$  SEM ( $n=3$ )



Comparisons of metabolic capacity in liver microsomes from mice

TOH, EROD and PROD activities in liver microsomes from CD-1 and nude mice are shown in Fig. 2 and Table 2, respectively. In these experiments, enzymatic activities were measured using relatively high concentrations ( $[S] \gg K_m$ ) and therefore these data are assumed to be indicative of the metabolic capacity. No significant differences between the strains were observed. The overall hydroxylation rate of testosterone, and also the hydroxylation at specific positions of testosterone, were very similar.

#### Conjugation of 7-HC by mouse liver slices

The  $CL_{int}$  of 7-HC ( $1 \mu M$ ) and the formation of 7-HC metabolites ( $50 \mu M$ ) are shown in Table 3. Incubation with 7-HC ( $50 \mu M$ ) gave rise to both sulfate and glucuronic acid conjugates. 7-HC was preferentially conjugated with glucuronide, which is in agreement with the results of Steensma et al. [18]. There were no significant differences observed in the depletion rate or  $CL_{int}$  of

7-HC or in the formation of 7-HC conjugates in liver slices between CD-1 and nude mice.

#### Detection of cyp and efflux transporter mRNA levels

In both strains, the major cyp isoforms present in liver tissues were cyp1a2 and cyp3a11, whereas cyp1a1 and cyp2b10 were predominantly expressed in the upper part of the intestinal tract (Table 4). The expression levels of cyp1a1, cyp1a2, cyp2b10 and cyp3a11 in kidney, colon and adrenal glands were low or even absent (Table 4). The efflux transporter mdr1a was highly expressed in adrenal glands and in the intestinal tract of both strains, and the levels increased from the duodenum towards the colon (Table 5). In the kidney the major transporters present were mrp1 and mrp2, whereas in the liver, mrp2 was expressed at significant levels. Mdr1b was detected at high levels in the adrenal glands (Table 5).

The cyp and transporter mRNA expression profiles for both strains in all organs evaluated were very similar. The only significant difference between species was observed with respect to cyp1a1, which was found to be expressed at levels three times higher in the duodenum of nude mice.

**Table 2** EROD and PROD activities in liver microsomes of CD-1 and nude mice. The values presented are means  $\pm$  SEM ( $n=3$ )

Mouse strain	Activity (pmol/min/mg)	
	EROD	PROD
CD-1	125.5 $\pm$ 4.2	16.8 $\pm$ 0.5
Nude	113.5 $\pm$ 2.0	13.6 $\pm$ 0.3

**Table 3** Metabolism of 7-HC in liver slices from CD-1 and nude mice. The values presented are means  $\pm$  SEM ( $n=6$  slices) from two separate experiments

	CD-1 mouse	Nude mouse
$CL_{int}$ (ml/min/mg)	5.7 $\pm$ 0.7	7.9 $\pm$ 0.8
7-HC sulfate (pmol/min/mg)	64.0 $\pm$ 15.6	91.7 $\pm$ 9.6
7-HC glucuronide (pmol/min/mg)	128.0 $\pm$ 17.0	111.0 $\pm$ 23.0

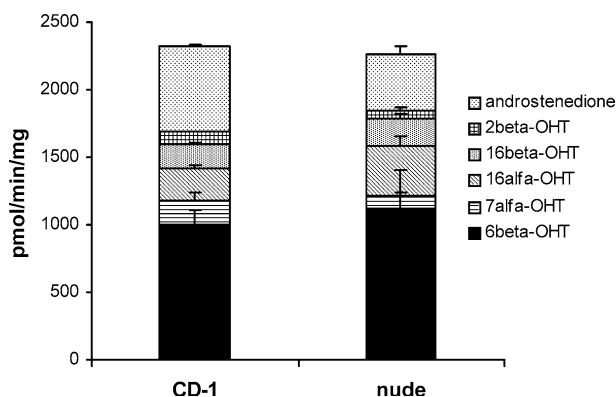


**Fig. 2** TOH activity in liver microsomes of CD-1 and nude mice. The data presented are means  $\pm$  SEM ( $n=3$ )

**Table 4** Relative mRNA expression level of *cyp1a1*, *cyp1a2*, *cyp2b10* and *cyp3a11* in liver, kidney, duodenum, ileum, colon and adrenal glands of CD-1 and nude mice. Total RNA (3.5 ng) was loaded for one-step real-time RT-PCR assay and the levels of *cyp* mRNA were expressed as ratios in relation to the levels of  $\beta$ -actin

Tissue	CD-1 mice				Nude mice			
	<i>cyp1a1</i>	<i>cyp1a2</i>	<i>cyp2b10</i>	<i>cyp3a11</i>	<i>cyp1a1</i>	<i>cyp1a2</i>	<i>cyp2b10</i>	<i>cyp3a11</i>
Liver	+	++++	++	++++	+	++++	++	++++
Kidney	—	+	+	+	—	+	+	+
Duodenum	+++	—	++++	+	++++	—	++++	+
Ileum	++	—	++	+	++	—	++	+
Colon	—	—	—	—	—	—	—	—
Adrenal glands	—	—	—	—	—	—	—	—

\* $P < 0.05$

**Table 5** Relative mRNA expression level of *mdr1a1*, *mdr1b*, *mrp1* and *mrp2* in liver, kidney, duodenum, ileum, colon and adrenal glands of CD-1 and nude mice. Total RNA (3.5 ng) was loaded for one-step real-time RT-PCR assay and the levels of *cyp* mRNA were expressed as ratios in relation to the levels of  $\beta$ -actin mRNA,

which was used to normalize RNA loading. Results are the mean from three animals (+ to ++++ indicate increasing levels of mRNA expression, and — indicates undetectable or no signal, after more than 35 PCR cycles)

Tissue	CD-1 mice				Nude mice			
	<i>mdr1a</i>	<i>mdr1b</i>	<i>mrp1</i>	<i>mrp2</i>	<i>mdr1a</i>	<i>mdr1b</i>	<i>mrp1</i>	<i>mrp2</i>
Liver	+	—	+	++++	++	—	+	++++
Kidney	++	+	+++	+++*	++	+	+++	+++
Duodenum	++++	—	+	+++*	++++	—	+	++
Ileum	+++++	—	+	+	+++++	—	+	+
Colon	+++++	—	++	—	+++++	—	++	—
Adrenal glands	++++	++++	++++	—	++++	++++	++++	—

\* $P < 0.05$

## Discussion

In oncology drug discovery and development, the athymic nude mouse is a very useful investigation model due to its ability to support the growth of tumors of human origin. On the other hand, and at the same time, pharmaceutical industries are using extensively CD-1 mice to investigate the toxicity and pharmacokinetic behavior of new chemical entities. Linking the efficacy data obtained in nude mice to the pharmacokinetic parameters obtained in CD-1 mice, raises the question as to whether the metabolic and pharmacokinetic characteristics of xenobiotics in these strains are comparable or not. Moreover, pharmacokinetic data from CD-1 mice may be used to build a pharmacokinetic/pharmacodynamic model in order to elucidate the relationship between drug exposure and tumor growth inhibition in nude mice. Therefore, the purpose of this study was to characterize these two mice strains with respect to their drug metabolism and drug transporter properties. Only the male mouse was investigated because it is predominantly used in toxicological studies. Hepatic phase I and phase II metabolism of a set of well-known drugs and the enzymatic activities towards testosterone, ethoxyresorufin and pentoxyresorufin were investigated. The results clearly demonstrate close similarity between the two strains.

In addition, mRNA levels of major *cyp* isoforms and drug efflux transporters were investigated by real-time RT-PCR in the liver, kidney, intestine and adrenal glands of both strains. *Cyp1a2* and *cyp3a11* were significantly expressed in the liver, but no, or only weak, expression was observed in other tissues. Similar findings have been reported previously for BALB/c mice [5]. On the other hand, *cyp1a1* and *cyp2b10* were found to be expressed extrahepatically, mainly in the duodenum and ileum. In a recent study, constitutive mRNA levels of *cyp1a1* and *cyp2b10* have also been detected in small intestines of B6 mice, and can be induced by  $\beta$ -naphthoflavone and phenobarbital, respectively [22]. In this study, no marked differences were detected between the two strains, except for *cyp1a1*, the expression of which was significantly higher (threefold) in nude mouse duodenum. However, it should be mentioned that a threefold increase in *cyp1a1* mRNA expression is relatively small and, in general, reflects an even smaller change in protein activity. For example, in rats treated with Aroclor, induction of CYP1A1 gave rise to about a 23,000-fold induction of mRNA level, but only to a 127-fold difference in protein activity [11]. It can be hypothesized that the difference in duodenal *cyp1a1* mRNA expression is due to the fact that nude mice are not exposed to bacteria, and bacteria-derived factors such as LPS. Both bacteria and LPS are well known for

their ability to downregulate CYP isoforms [14]. Regarding the drug transporter genes, *mdr1a* was highly expressed in the intestine and adrenal glands of both strains. An interesting observation in this study was the increasing expression level of *mdr1a* going from duodenum towards colon. Previously, several other groups have also reported the intestinal expression of *mdr1a* in mice, both at the level of mRNA and protein [13, 15, 16].

High expression levels of *mdr1b* have been detected previously in the adrenal gland, pregnant uterus and ovaries of mice [6]. The current study confirmed the adrenal gland-specific expression of *mdr1b*, as weak or no *mdr1b* mRNA gene expression was detected in liver, kidney and intestinal tissue.

The expression of *mrp2* was high in liver and kidney, and only weak or no expression was detected in the intestine and the adrenal glands. *Mrp1* could be detected in all tissues, with the highest expression in kidney and adrenal glands. Using another mouse strain (C57/BL6), similar profiles for *mrp1* and *mrp2* have been described previously [23]. Despite the fact that the expression of drug-metabolizing enzymes and drug transporters have been studied in different tissues and in different animals, including mice, this is the first study in which two mice strains, commonly used in oncology discovery and development, have been characterized for their hepatic drug metabolism and drug transporters properties.

In conclusion, CD-1 and athymic nude mice demonstrate remarkable similarities in mRNA expression of major drug-metabolizing enzymes and efflux transporters in all organs. The comparison of cyp expression between CD-1 and nude mice is also reflected in the close similarity of enzymatic activities between the two strains. Therefore, the potential error in extrapolating pharmacokinetic data obtained from CD-1 to nude mice, or vice versa, is expected to be minimal.

**Acknowledgement** The authors are grateful to Dr. Peter Buchan for critical reading of the manuscript.

## References

1. Ayrton A, Morgan P (2001) Role of transport proteins in drug absorption, distribution and excretion. *Xenobiotica* 31:469–497
2. Borst P, Schinkel AH (1996) What have we learnt thus far from mice with disrupted P-glycoprotein genes? *Eur J Cancer* 32A:985–990
3. Bradford MM (1976) A rapid and sensitive method for the quantitation of microgram quantities of protein utilizing the principle of protein-dye binding. *Anal Biochem* 72:248–254
4. Busby WF Jr, Ackermann JM, Crespi CL (1999) Effect of methanol, ethanol, dimethyl sulfoxide, and acetonitrile on in vitro activities of cDNA-expressed human cytochromes P-450. *Drug Metab Dispos* 27:246–249
5. Choudhary D, Jansson I, Schenkman JB, Sarfarazi M, Stoilov I (2003) Comparative expression profiling of 40 mouse cytochrome P450 genes in embryonic and adult tissues. *Arch Biochem Biophys* 414:91–100
6. Croop JM, Raymond M, Haber D, Devault A, Arceci RJ, Gros P, Housman DE (1989) The three mouse multidrug resistance (*mdr*) genes are expressed in a tissue-specific manner in normal mouse tissues. *Mol Cell Biol* 9:1346–1350
7. De Kanter R, Monshouwer M, Draaisma AL, De Jager MH, de Graaf IA, Proost JH, Meijer DK, Groothuis GM (2004) Prediction of whole body metabolic clearance of drugs through the combined use of slices from rat liver, lung, kidney, small intestine and colon. *Xenobiotica* 34:229–241
8. Kelland LR (2004) Of mice and men: values and liabilities of the athymic nude mouse model in anticancer drug development. *Eur J Cancer* 40:827–836
9. Manzotti C, Audisio RA, Pratesi G (1993) Importance of orthotopic implantation for human tumors as model systems: relevance to metastasis and invasion. *Clin Exp Metastasis* 11:5–14
10. Martignoni M, Monshouwer M, de Kanter R, Pezzetta D, Moscone A, Grossi P (2004) Phase I and phase II metabolic activities are retained in liver slices from mouse, rat, dog, monkey and human after cryopreservation. *Toxicol In Vitro* 18:121–128
11. Meredith C, Scott MP, Renwick AB, Price RJ, Lake BG (2003) Studies on the induction of rat hepatic CYP1A, CYP2B, CYP3A and CYP4A subfamily form mRNAs in vivo and in vitro using precision-cut rat liver slices. *Xenobiotica* 33:511–527
12. Mizuno N, Niwa T, Yotsumoto Y, Sugiyama Y (2003) Impact of drug transporter studies on drug discovery and development. *Pharmacol Rev* 55:425–461
13. Mochida Y, Taguchi K, Taniguchi S, Tsuneyoshi M, Kuwano H, Tsuzuki T, Kuwano M, Wada M (2003) The role of P-glycoprotein in intestinal tumorigenesis: disruption of *mdr1a* suppresses polyp formation in *Apc(Min/+)* mice. *Carcinogenesis* 24:1219–1224
14. Pan J, Xiang Q, Ball S (2000) Use of a novel real-time quantitative reverse transcription-polymerase chain reaction method to study the effects of cytokines on cytochrome P450 mRNA expression in mouse liver. *Drug Metab Dispos* 28:709–713
15. Schinkel AH, Smit JJ, van Tellingen O, Beijnen JH, Wagenaar E, van Deemter L, Mol CA, van der Valk MA, Robanus-Maandag EC, te Riele HP, et al (1994) Disruption of the mouse *mdr1a* P-glycoprotein gene leads to a deficiency in the blood-brain barrier and to increased sensitivity to drugs. *Cell* 77:491–502
16. Schinkel AH, Mayer U, Wagenaar E, Mol CA, van Deemter L, Smit JJ, van der Valk MA, Voordouw AC, Spits H, van Tellingen O, Zijlmans JM, Fibbe WE, Borst P (1997) Normal viability and altered pharmacokinetics in mice lacking *mdr1*-type (drug-transporting) P-glycoproteins. *Proc Natl Acad Sci U S A* 94:4028–4033
17. Smit JW, Schinkel AH, Weert B, Meijer DK (1998) Hepatobiliary and intestinal clearance of amphiphilic cationic drugs in mice in which both *mdr1a* and *mdr1b* genes have been disrupted. *Br J Pharmacol* 124:416–424
18. Steensma A, Beamand JA, Walters DG, Price RJ, Lake BG (1994) Metabolism of coumarin and 7-ethoxycoumarin by rat, mouse, guinea pig, cynomolgus monkey and human precision-cut liver slices. *Xenobiotica* 24:893–907
19. Weaver RJ (2001) Assessment of drug-drug interactions: concepts and approaches. *Xenobiotica* 31:499–538
20. Xie H, Audette C, Hoffee M, Lambert JM, Blattler WA (2004) Pharmacokinetics and biodistribution of the antitumor immunoconjugate, cantuzumab mertansine (huC242-DM1), and its two components in mice. *J Pharmacol Exp Ther* 308:1073–1082
21. Yamazaki M, Suzuki H, Sugiyama Y (1996) Recent advances in carrier-mediated hepatic uptake and biliary excretion of xenobiotics. *Pharm Res* 13:497–513
22. Zhang QY, Dunbar D, Kaminsky LS (2003) Characterization of mouse small intestinal cytochrome P450 expression. *Drug Metab Dispos* 31:1346–1351
23. Zollner G, Fickert P, Fuchsichler A, Silbert D, Wagner M, Arbeiter S, Gonzalez FJ, Marschall HU, Zatloukal K, Denk H, Trauner M (2003) Role of nuclear bile acid receptor, FXR, in adaptive ABC transporter regulation by cholic and ursodeoxycholic acid in mouse liver, kidney and intestine. *J Hepatol* 39:480–488